Research Article

SOHAG JOURNAL OF SCIENCES

https://doi.org/10.21608/sjsci.2023.218511.1088

Synthesis and Antimicrobial Activity of Novel Bisbenzoxazine Monomer

Ahmed Soliman[1], Kamal I. Aly[2], Amer A. Amer[1], Ahmed E. Abdel-Aziz[3], Mohamed Gamal Mohamed[2,4*] and Mostafa R. Belal[1*]

[1] *Department of Chemistry, Faculty of Science, Sohag University, Sohag 82524, Egypt.*
[2] *Polymer Research Laboratory, Chemistry Department, Faculty of Science, Assiut University, Assiut 71516, Egypt.*
[3] *Department of Botany and Microbiology, Faculty of Science, New Valley University, El-Kharga 72511, Egypt.*
[4] *Department of Materials and Optoelectronic Science, College of Semiconductor and Advanced Technology Research, Center for Functional Polymers and Supramolecular Materials, National Sun Yat-Sen University, Kaohsiung, 804, Taiwan.*
**Email: (M.G.M: mgamal.eldin12@aun.edu.eg, M.R.B:mostafarabie2022@science.sohag.edu.eg)*

Received: 20th June 2023 **Revised:** 26th July 2023 **Accepted:** 8th August 2023
Published online: 1st September 2023

Abstract: In this research, a compound called 2,2'-((1E,1'E)-(hexane-1,6-diylbis(azanylylidene))bis(methanylylidene))diphenol (SA-HMDASF) was synthesized by combining salicylaldehyde and hexamethylene diamine. The resulting SA-HMDASF was then reduced using sodium borohydride, leading to the formation of 2,2'-((hexane-1,6-diylbis((SA-HMDA-NH) through a chemical reaction. Subsequently, SA-HMDA-NH was reacted with formaldehyde, resulting in the production of a benzoxazine monomer called SA-HMDA-BZ. To determine the chemical composition of SA-HMDA-BZ, different analytical methods such as FT-IR, ^{1}H, and ^{13}C NMR spectroscopy were employed. These methods were crucial in identifying and confirming the molecular composition and arrangement of the compound. Furthermore, Scanning Electron Microscopy (SEM) was used to analyze the surface morphology of SA-HMDA-BZ while its crystalline properties were assessed through X-ray Diffraction (XRD) analysis. These characterization techniques provided valuable insights into the physical attributes and structural properties of SA-HMDA-BZ. Additionally, the antimicrobial activity of SA-HMDA-BZ was investigated, and the results displayed promising outcomes. The compound exhibited notable antimicrobial properties, suggesting its potential as an effective agent against various microorganisms.
Keywords: Benzoxazine, Crystallinity, Thermal stability, and Antimicrobial activity.

1. Introduction

Benzoxazine (BO) has received a lot of interest lately because it has numerous benefits over conventional phenolic resins. BO offers a range of beneficial properties, including a low dielectric value, minimal water intake, excellent thermal durability, high resistance to chemicals, and little shrinking during the healing process [1,2]. The use of bisphenol A (BPA) in the synthesis of benzoxazine has been widely discussed in the literature. Compared to thermoset resins derived from novolac and epoxy resins of the BPA type, the resulting cured BO resin exhibits superior qualities including higher thermal resistance, superb electric current insulation, and improved water durability [3,4]. However, it is worth noting that BPA has been associated with various health concerns, including cardiovascular disease, type 2 diabetes, and changes in liver enzymes, as indicated by several studies. One of the most significant advancements in the field of therapeutics lies in the development of potent and effective antimicrobial agents. These agents have played a vital role in preventing and treating infectious complications that may arise from various therapy methods, including radiation for cancer, operations, and infections. Moreover, they have proven instrumental in controlling severe infections [5]. Researchers conducted the development of benzoxazine as a promising new medication. These compounds belong to a significant class of benzo-fused heterocycles that exhibit diverse biological functions. According to reports, benzoxazines demonstrate properties such as D2 receptor antagonism, analgesic effects, antimicrobial activity, anti-inflammatory properties, and antioxidant capabilities [5-9]. The Benzoxazine nucleus has been known to exhibit significant antimicrobial activity against both bacteria and fungi. Given that the newly synthesized SA-HMDA-BZ also contains the same Benzoxazine nucleus, we conducted antimicrobial activity tests to determine whether it retains the same potent antimicrobial properties as its predecessor [10-14]. Aminomethyl derivatives of benzoxazine have shown potential for use as anticancer, antibacterial, analgesic, and anti-inflammatory agents [15-17]. Previously, an Indonesian research group reported the synthesis of benzoxazine derivatives and certain aminomethyl derivatives of eugenol through the Mannich reaction. Further investigation is warranted to explore the anticancer potential and bioactivity of these aminomethyl and benzoxazine derivatives of eugenol [18,19]. The compounds displayed remarkable anticancer activity in the brine shrimp lethality test (BST), highlighting the need for additional research to evaluate their bioactivity [20]. Levulinic acid and phenol are synthesized chemically to produce diphenolic acid (DPA), also known as 4,4'-bis(4-hydroxyphenyl)pentanoic acid, in the presence of a promoter. Levulinic acid is regarded Levulinic acid is considered a building block chemical with a cost-effective platform chemical that can be developed on a large scale from cellulose-

rich biomass, particularly waste wood biomass. DPA offers several advantages over bisphenol A (BPA), including lower cost, a similar chemical structure to BPA, and an additional carboxylic acid functionality that can be utilized in polymer manufacturing. Therefore, DPA presents a viable alternative to BPA in the synthesis of polybenzoxazine compounds [21]. Benzoxazines exhibit a wide range of biological activities, making them important molecules for the development of various pharmaceutical agents, such as antifungals and antimicrobials [22]. Herein, we successfully synthesized a new benzoxazine monomer known as SA-HMDA-BZ. The synthesis involved the condensation of hexamethylene diamine (HMDA) with salicylaldehyde (SA) through a Schiff base reaction. The resulting Schiff base compound was then reduced using sodium borohydride, followed by closing the ring with formaldehyde (37%) in 1,4-dioxane (DO) at 100 °C [**Fig. 1**]. To confirm the chemical structures of the synthesized SA-HMDA-BZ monomer, we employed techniques such as proton and carbon nuclear magnetic resonance spectroscopy (1H and 13C), and Fourier-transform infrared spectroscopy (FTIR). Scanning electron microscopy (SEM) and X-ray diffraction (XRD) were employed to analyze the morphology and crystallinity, respectively of SA-HMDA-BZ. Furthermore, we studied SA-HMDA-BZ's antibacterial properties, which exhibited promising results.

2. Materials and methods

2.1. Materials

Salicylaldehyde (SA), hexamethylene diamine (HMDA), Acros Organics in Belgium provided the following materials: ethanol, sodium hydroxide (NaOH), anhydrous sodium sulfate, formaldehyde (37%), 1,4-dioxane (DO), sodium borohydride ($NaBH_4$), and chloroform. All of the used chemicals and solvents in this experiment were acquired from Sigma-Aldrich and were of analytical quality. They were utilized in their original form without any further processing.

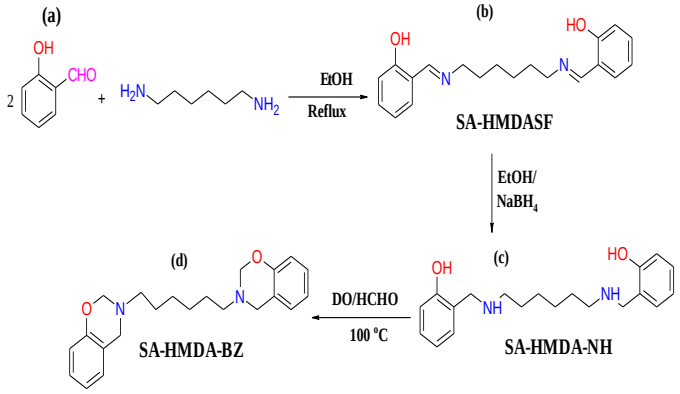

Figure 1: SA-HMDASF (b), SA-HMDA-NH (c), and SA-HMDA-BZ (d) were synthesized from SA (a).

2.2. Synthesis of 2,2'-((1E,1'E)-(hexane-1,6-diylbis(azanylylidene)) bis(methanylylidene)) diphenol [SA-HMDASF].

Individually, salicylaldehyde (80 mmol, 8.34 mL) and hexamethylene diamine (40 mmoles, 5 mL) exhibited miscibility in 40 mL absolute ethanol. SA and HMDA were combined in a 2:1 molar ratio, respectively slowly and stirred for a duration of 5 hours at 60 °C. As a result of the reaction, a yellow solid product was obtained as yield (86%), crystallized in methanol with m.p: 74-75 °C. FTIR (KBr, cm^{-1}): 3600–3400 (OH), 1632 (CH=N). ^{1}H-NMR (400 MHz, DMSO-d_6, δ, ppm): 13.55 (s, 2H, -OH), 8.50 (s, 2H, -CH=N-), 6.70–7.50 (m, 8H, ArH), 3.60 (t, 4H, **a**), 1.65 (m, 4H, **b**), 1.41 (m, 4H, **c**). ^{13}C-NMR (100 MHz, DMSO-d_6, δ, ppm): on decoupled 166 (2C, -CH=N-), 116-163 (12C aromatic) which become (8C aromatic) on dept due to 4C had no proton and peaks (**a**, **b** and **c**) directed to down at (59, 31, 27), respectively. HRMS (ESI): calcd. For $C_{20}H_{24}O_2N_2$ 324.1191 [M+]; found 324.1204.

2.3. Synthesis of 2,2'-((hexane-1,6-diylbis(azanediyl))bis(methylene))diphenol [SA-HMDA-NH].

For the reduction reaction, SA-HMDASF (20 mmol, 6.48 g) was stirred in 30 mL abs. ethanol while slowly adding sodium borohydride (0.76 g) over a period of three hours. Using Thin-layer chromatography (TLC) to monitor the completion of the reduction process. Following this, 100 mL of water was added, and the resulting product was extracted using chloroform. The organic phase was then washed with water, dried using anhydrous sodium sulfate, and finally concentrated to dryness using a vacuum. As a result, a white solid product was obtained after crystallization in ethanol (yield: 72%) with m.p: 113-114 °C. FTIR (KBr, cm^{-1}): 3274 (NH, stretching), 3200–3550 (OH, broad) due to hydrogen bond, 1589 (-NH-, bending). ^{1}H-NMR (400 MHz, DMSO-d_6, δ, ppm): 8.30 (s, 2H, OH), 6.6–7.20 (m, 8H, ArH), 4.20 (s, 2H, NH), 3.82 (s, 4H, d), 2.50 (t, 4H, **a**), 1.45 (m, 4H, **b**), 1.27 (m, 3H, **c**). ^{13}C-NMR (100 MHz, DMSO-d_6, δ, ppm): on dept 116-138 which become (8C aromatic) due to 4C had no proton and peaks (**a**, **b**, **c** and **d**) directed to down at (65, 59, 31, 27), respectively. HRMS (ESI): calcd. For $C_{20}H_{28}O_2N_2$ 328.2131 [M+]; found 328.2402.

2.4. Synthesis of SA-HMDA-BZ.

An extra amount of formaldehyde (32 mmol, 1.14 mL) was mixed into an SA-HMDA-NH (30 mmol (24 %), 9.84 g) in 30 mL of DO at a temperature of 100 °C for a duration of 27 hours. Using Thin-layer chromatography (TLC) to monitor the completion of the reaction process. After the reaction, the residue was collected and dissolved in chloroform and subjected to washing with a 2 M NaOH solution (20 mL) immediately after evaporating the solvent. The organic layer was then dried over sodium sulfate and concentrated to dryness using a vacuum. The final product obtained was a gray solid (yield: 72%) and crystallized in methanol. FTIR (KBr, cm^{-1}), 1233 (COC antisymmetric stretching), 1107 (COC symmetric stretching), and 935 (oxazine ring). ^{1}H-NMR (400 MHz, DMSO-d_6, δ, ppm): 6.60–7.20 (m, 8H, ArH), 4.43 (s, 4H, **f**), 3.82 (s, 4H, **e**), 2.50 (t, 4H, **a**), 1.45 (m, 4H, **b**), 1.27 (m, 4H, **c**). ^{13}C NMR (100 MHz, $CDCl_3$, δ, ppm): on dept 116-138 (8C aromatic) which become (8C aromatic), and peaks (**f**, **e**, **a**, **b**, **c** and **d**) directed down at (82, 65, 59, 31, 27), respectively. **Table 1** presented a list of SA-HMDA-BZ's physical characteristics. HRMS (ESI): calcd. For $C_{22}H_{28}O_2N_2$ 352.2133

[M+]; found 352.2226.

2.5. Antimicrobial activities.

To evaluate the antimicrobial activity of SA-HMDA-BZ, different concentrations (625, 1250, 2500, 5000, and 10000 ppm) were tested using the agar well diffusion assay method [23]. The recommended concentration for standard antibacterial agents is typically the minimum inhibitory concentration specified by the manufacturer. The antimicrobial activities of the selected compounds were assessed against various microorganisms, including *Aspergillus fumigatus*, Cryptococcus neoformans, Candida albicans, Syncephalastrum racemosum *Staphylococcus aureus*, *Bacillus subtilis*, *Pseudomonas aeruginosa*, and *Escherichia coli*. *Ampicillin* and *gentamycin* were used as standard antibacterial agents, while amphotericin B served as the standard antifungal agent. By measuring the average diameter of those inhibiting zones surrounding the wells (in millimeters), compared to the reference medications, the reactivity of the microbiological isolates to the substance being studied chemicals was determined.

3. Results and Discussion:

3.1. Synthesis and characterization of SA-HMDA-BZ

In this study, salicylaldehyde (SA) and hexamethylene diamine (HMDA) were employed to synthesize SA-HMDASF [**Fig. 1(b)**]. The resulting SA-HMDASF was further subjected to reduction using $NaBH_4$, leading to the formation of SA-HMDA-NH [**Fig. 1(c)**]. Subsequently, SA-HMDA-NH underwent a reaction with CH_2O, resulting in the synthesis of a novel benzoxazine precursor known as SA-HMDA-BZ. It is noteworthy that this reaction was accomplished without the need for any catalyst [**Fig. 1(d)**].

Table 1: List of SA-HMDA-BZ's physical characteristics.

Physical Properties	SA-HMDA-BZ
State	Solid, melting point: 183 ºC
Color	Gray
Solubility (H_2O)	Insoluble
Solvent	DMSO

Fig. 2(a) shows an FTIR spectrum of SA-HMDASF, exhibiting characteristic absorption peaks. The hydroxyl group was shown by the peak in the range of 3600-3400 cm^{-1}, while the CH=N group was shown by the peak at 1632 cm^{-1}. Furthermore, **Fig. 2(b)**'s peaks at 3274 cm^{-1} (NH stretching) and 1589 cm^{-1} (NH bending) show that SA-HMDASF was effectively reduced. This was further amplified by the peak at 1632 cm^{-1}, which is linked with the CH=N group, disappearing in **Fig. 2(b)**. The FTIR spectrum of SA-HMDA-BZ in **Fig. 2(c)** observed peaks at 1233 cm^{-1}, 1107 cm^{-1}, and 935 cm^{-1} correspond to asymmetric, symmetric stretching of the C-O-C unit and the oxazine ring, respectively. The ^1H NMR spectrum of SA-HMDASF, shown in **Fig. 3(a)**, showed characteristic signals at 13.55 ppm for the OH group, while signals at 8.50 ppm and 6.70-7.50 ppm were attributed to the CH=N and aromatic protons, respectively. Additionally, signals at 3.60 ppm, 1.65 ppm, and 1.41 ppm are observed for the (a, b, c) groups. In the case of SA-HMDA-NH, depicted in **Fig. 3(b)**, the ^1H NMR spectrum displays signals at 8.30 ppm for the OH group, 6.6-7.20 ppm for the aromatic protons, 4.20 ppm for the NH group, and 3.82 ppm, 2.50 ppm, 1.45 ppm, and 1.27 ppm for the (d, a, b, c) groups. The existence of the NH band shows that SA-HMDASF was successfully reduced to SA-HMDA-NH. Furthermore, **Fig. 3(c)** SA-HMDA-BZ, exhibits signals at 6.60-7.20 ppm for the aromatic protons (f, e), 4.43 ppm for the (b) group, and 3.82 ppm, 2.50 ppm, 1.45 ppm, and 1.27 ppm for the (a, b, c) groups, respectively. These signals indicate evidence of ring-closing in the formation of SA-HMDA-BZ. The ^{13}C NMR spectrum of SA-HMDASF, illustrated in **Fig. 4(a)**, exhibits characteristic signals. The signal at 166 ppm corresponds to the (CH=N) carbon nuclei, In addition, signals in the range of 116-163 ppm are observed for the aromatic carbon nuclei, indicating occur underwent Mannich condensation reactions between SA-HMDASF and SA and the appearance of peaks (a, b, and c) at downfield positions (59 ppm, 31 ppm, and 27 ppm, respectively). In the ^{13}C NMR spectrum of SA-HMDA-NH shown in **Fig. 4(b)**, the carbon nuclei of the aromatic carbon appear in the range of 138.00-116.00 ppm, denoted as (8C aromatic) due to the absence of protons and peaks on the corresponding carbons. Additionally, signals (d, a, b, and c) are observed at downfield positions (65 ppm, 59 ppm, 31 ppm, and 27 ppm, respectively). The presence of the signal (d) at 65 ppm indicates the successful reduction of SA-HMDASF, resulting in the formation of SA-HMDA-NH. Furthermore, in the ^{13}C NMR spectrum of SA-HMDA-BZ depicted in **Fig. 4(c)**, signals are observed for aromatic carbon in the range of 138.00-116.00 ppm. Additionally, signals (f, e, a, b, c, and d) are observed at downfield positions (82 ppm, 65 ppm, 59 ppm, 31 ppm, 27 ppm, and 27 ppm, respectively). The signal (f) indicates the ring-closing process, suggesting the formation of a benzoxazine monomer. Regarding crystalline properties were assessed through X-ray Diffraction (XRD) profiles, SA-HMDA-BZ exhibits a signal at $2\theta = 19°$, which corresponds to the (002) plane. This signal indicates the presence of irregular and amorphous carbons, as shown in **Fig. 5**. Additionally, the surface morphology of SA-HMDA-BZ was analyzed using Scanning Electron Microscopy (SEM), revealing a flower pattern, as depicted in **Fig. 6**. These characterization techniques (SEM and XRD) offered valuable insights into the physical attributes and structural properties of SA-HMDA-BZ. Moreover, the SEM and XRD analyses played a crucial role in evaluating the feasibility of utilizing SA-HMDA-BZ as an anti-corrosion coating for metals by indicating its mobility and potential effectiveness in such applications.

3.2. Antimicrobial activities of SA-HMDA-BZ

SA-HMDA-BZ displayed variable antimicrobial activity across different organisms. As the compounds' concentration increased, the tested compounds' effectiveness against the microbes also increased. Among the compounds evaluated for their impact on gram-positive and gram-negative bacteria, SA-HMDA-BZ exhibited the highest potency.

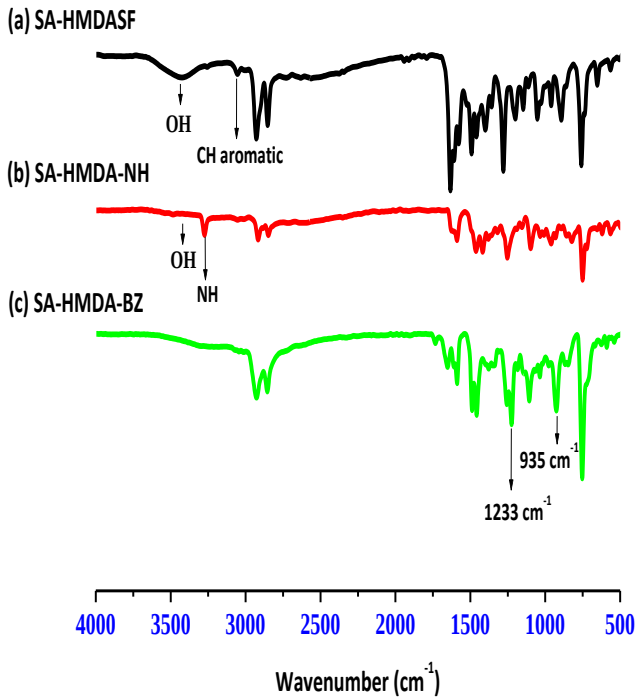

Figure 2: FTIR spectra of (a) SA-HMDASF, (b) SA- HMDA-NH, (c) SA- HMDA-BZ.

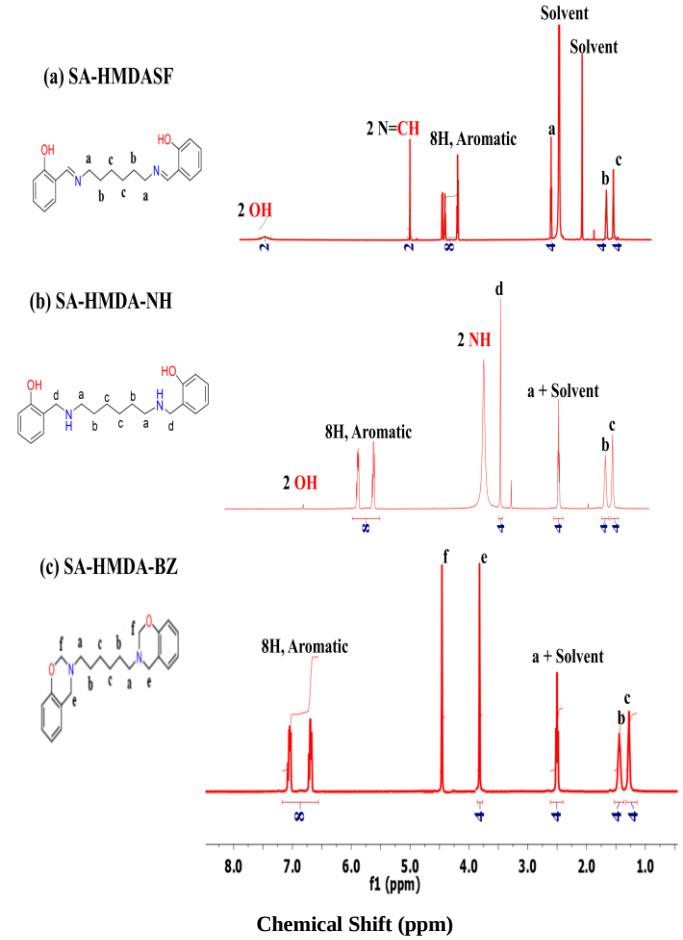

Figure 3: ^{1}H NMR of (a) SA-HMDASF, (b) SA-HMDA-NH, and (c) SA-HMDA-BZ.

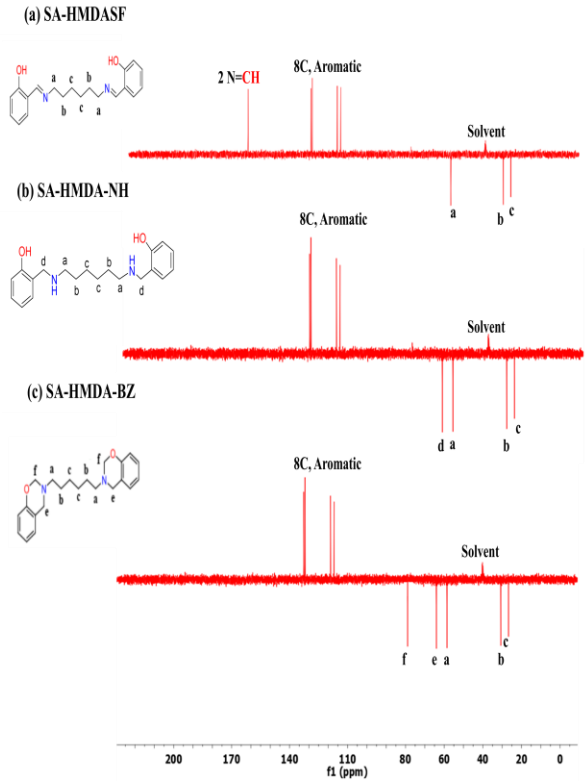

Figure 4: ^{13}C NMR of (a) SA-HMDASF, (b) SA-HMDA-NH and (c) SA-HMDA-BZ.

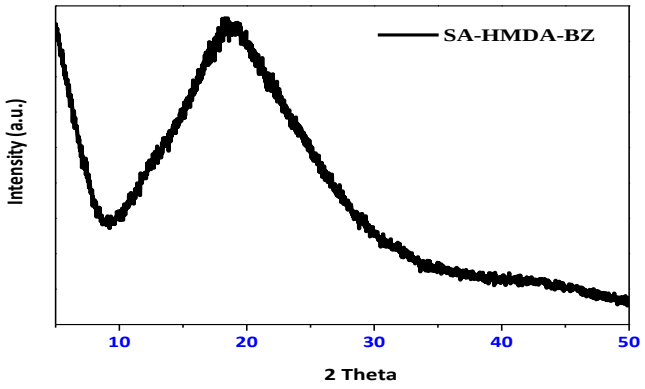

Figure 5: XRD Pattern of SA-HMDA-BZ.

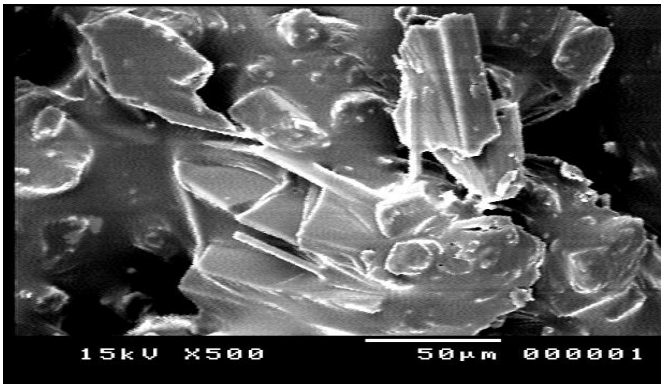

Figure 6: SEM morphology of SA-HMDA-BZ at magnification (X500).

At a concentration of 10000 ppm, it achieved remarkable results, resulting in inhibition zones of 83.9% and 81.9% against gram-positive bacteria (*Bacillus subtilis* and *Staphylococcus aureus*, respectively) and 75.9% and 72.3% against gram-negative bacteria (Escherichia coli and Pseudomonas aeruginosa, respectively). Additionally, at a concentration of 5000 ppm, SA-HMDA-BZ demonstrated a significant effect on gram-positive bacteria, as indicated in **Table 2**. In **Table 3**, SA-HMDA-BZ at various concentrations exhibited moderate to mild activity against fungal species. **Table 2 and Table 3** clearly demonstrate the use of ampicillin and gentamicin as standard antibacterial agents, along with amphotericin B as the standard antifungal agent.

Table 2: Antibacterial activity of SA-HMDA-BZ compounds (diameter of inhibition zone in mm).

Tested microorganisms		Fungi Inhibition zone diameter in mm and (%) value			
		Aspergillus fumigatus	*Syncephalastrum racemosum*	*Candida albicans*	*Cryptococcus neoformans*
		Amphotericin B			
Comp.	Conc. (ppm)	20.2 ± 0.1	18.2 ± 0.2	21.9 ± 0.1	22.7 ± 0.2
SA-HMDA-BZ	625	0.8 ± 0.2 (3.9%)	0.8 ± 0.4 (4.4%)	0.7 ± 0.4 (3.2%)	0.8 ± 0.7 (3.5%)
	1250	1.9 ± 0.5 (9.4%)	1.3 ± 0.3 (7.1%)	1.7 ± 0.2 (7.8%)	1.2 ± 0.1 (5.3%)
	2500	3.3 ± 0.2 (16.3%)	2.9 ± 0.2 (15.9%)	3.0 ± 0.2 (13.7 %)	2.7 ± 0.3 (11.9%)
	5000	5.4 ± 0.2 (26.7%)	4.5 ± 0.4 (24.7%)	4.9 ± 0.2 (22.4%)	4.2 ± 0.9 (18.5%)
	10000	9.8 ± 0.4 (48.5%)	8.4 ± 0.5 (46.2%)	8.6 ± 0.6 (39.3%)	8.0 ± 0.1 (35.2%)

Table 3: Antifungal activity of SA-HMDA-BZ compounds (diameter of inhibition zone in mm).

Tested microorganisms		Gram positive bacteria inhibition zone diameter in mm and (%*) value		Gram negative bacteria inhibition zone diameter in mm and (%*) value	
		Staphylococcus aureus	*Bacillus subtilis*	*Pseudomonas aeruginosa*	*Escherichia coli*
		Ampicillin		Gentamicin	
Comp.	Conc. (ppm)	23.8 ± 0.2	32.4 ± 0.3	17.3 ± 0.1	19.9 ± 0.3
SA-HMDA-BZ	625	2.8 ± 0.3 (11.8%)	3.9 ± 0.2 (12.04%)	1.8 ± 0.3 (10.4%)	2.1 ± 0.2 (10.5%)
	1250	6.2 ± 0.7 (26.1%)	9.1 ± 0.5 (28.1%)	3.9 ± 0.2 (22.5%)	5.1 ± 0.1 (25.6%)
	2500	10.1 ± 0.6 (42.4%)	15.7 ± 0.6 (48.5%)	7.2 ± 0.5 (41.6%)	8.3 ± 0.4 (41.7%)
	5000	16.9 ± 0.3 (71.0%)	23.2 ± 0.5 (71.6%)	10.3 ± 0.1 (59.5%)	12.6 ± 0.8 (63.3%)
	10000	19.5 ± 0.1 (81.9%)	27.2 ± 0.8 (83.9%)	12.5 ± 0.5 (72.3%)	15.1 ± 0.5 (75.9%)

(%*): The percentage of the diameter of the inhibition zone (mm) that appeared on microbial culture at each concentration when using the tested compounds to the diameter of the inhibition zone that appeared on culture when using the standard antimicrobial agent. (Diameter of inhibition zone of the tested compounds/diameter of inhibition zone of the standard antimicrobial agent X 100).

4. Conclusion

The synthesis of the SA-HMDA-BZ monomer involved three main steps: condensation, reduction, and ring-closing process, as illustrated in **Figure 1**. To determine its chemical structure, FT-IR, ^{1}H NMR, and ^{13}C NMR spectroscopy techniques were employed. The surface morphology of SA-HMDA-BZ was examined using Scanning Electron Microscopy (SEM), while its crystallinity was analyzed through X-ray Diffraction (XRD). The antimicrobial activity of SA-HMDA-BZ was assessed, and it demonstrated significant effectiveness against Gram-positive, Gram-negative bacteria and fungi. Notably, SA-HMDA-BZ exhibited the highest potential at a concentration of 10000 ppm compared to the reference standards, showcasing its strong antimicrobial properties.

CRediT authorship contribution statement:

Ahmed Soliman: Supervision. Kamal I. Aly: Supervision. Amer A. Amer: Supervision. Ahmed E. Abdel-Aziz: Methodology, Conceptualization. Mohamed Gamal Mohamed: Investigation, Methodology, Data curation, Conceptualization, Supervision, Writing – original draft. Mostafa R. Belal: Investigation, Conceptualization, Methodology, Writing – original draft.

Data availability statement

The data used to support the findings of this study are available from the corresponding author upon request.

Declaration of competing interest

The authors declare that they have no known competing financial interests or personal relationships that could have appeared to influence the work reported in this paper.

Acknowledgments

The work was supported by the Science, Technology & Innovation Funding Authority (STDF) in Egypt as part of the research project (Project ID: 46993).

References

[1] C. X. Viet, T. M. Hoan, N. T. M. Nguyet, *Journal of Science and Technology*, 55 (2017) 63–69.
[2] K. I. Aly, M. G. Mohamed, O. Younis, M. H. Mahross, M. Abdel-Hakim, M. M. Sayed, *Progress in Organic Coatings*, 138 (2020) 105385.
[3] A. M. M. Soliman, K. I. Aly, M. G. Mohamed, A. A. Amer, M. R. Belal, Abdel-Hakim Mohamed, *Scientific Reports*, 13 (2023) 1-13.
[4] A. S. Jasim, K. H. Rashid, K. F. AL-Azawi, A. A. Khadom, *Results in Engineering*, 15 (2022) 100573.
[5] M. Akhter, A. Husain, N. Akhter, M. S. Y. Khan, *Indian Journal of Pharmaceutical Sciences*, 73 (2011) 101-1044.
[6] E. Erdag, *Journal of Pharmaceutical Research*, 32 (2021) 23-30.
[7] R. Sharma, R. K. Yadav, N. K. Sahu, M. Jain, S. Chaudhary, *Current Topics in Medicinal Chemistry*, 21 (2021) 1538-1571.

[8] M. G. Mohamed, T. S. Meng, S. W. Kuo, *Polymer*, 226 (2021) 123827.
[9] M. G. Mohamed, S-W. Kuo, *Macromolecules*, 53 (2020) 2420–2429.
[10] Q. Ma, X. Liu, H. Wang, Q. Zhuang, J. Qian, *Materials Today Chemistry*, 23 (2022) 100707.
[11] M. S. Muftah, *Journal of Pharmacognosy and Phytochemistry*, 9 (2020) 215-217.
[12] P. Imchen, B. K. Zhimomi, L. Longkumer, S. Tumtin, T. Swu, T. Phucho, *Journal of Heterocyclic Chemistry*, 57 (2020) 3394-3399.
[13] G. S. Putra, T. A. Yuniarta, A. Syahrani, M. Rudyanto, *International Journal of Pharma Research & Review*, 5 (2016), 1-11.
[14] O. M. O. Habib, H. M. Hassan, A El-Meka, *American Journal of Organic Chemistry*; 2 (2012) 45-51.
[15] M. Mbaba, S. D. Khanye, G. S. Smith, C. Biot, Comprehensive Organometallic Chemistry 4th Ed. Elsevier, Amsterdam, Netherlands, 2022.
[16] C-M. Huang, A-R Lee, P-H Kang, W-H Huang, *Journal of Medical Sciences*, 30 (2010) 41-46.
[17] A. Idhayadhulla, R. Kumar, A. A. Nasser, Manilal, *Journal of chemical and pharmaceutical research*, 3 (2010) 904-911.
[18] M. Rudyanto, T. Widiandani, A. Syahranti, International Journal of Pharmacy and Pharmaceutical Sciences, 7 (2015) 229-232.
[19] M. Rudyanto, J. Ekowati, T. Widiandani, A. Syahrani, Journal of Public Health in Africa, 14 (2023) 2511.
[20] M. G. Mohamed T-C Chen, S-W Kuo, *Macromolecules*, 54 (2021) 5866–5877.
[21] K. I. Aly, A. A. Amer, M. H. Mahross, A. M. M. Soliman, M. R. Belal, M. G. Mohamed, *Heliyon*, 9 (2023) e15976.
[22] M. S. Muftah, Journal of Pharmacognosy and Phytochemistry, 9 (2022) 215-217.
[23] S. Magaldi, S. Mata-Essayag, C. Hartung de Capriles, 8 (2004) 39–45.